DMD Fast Forward. Published on September 30, 2021 as DOI: 10.1124/dmd.121.000635
This article has not been copyedited and formatted. The final version may differ from this version.

Characterization of cytosolic glutathione-S- transferases (GSTs) involved in the metabolism of the aromatase inhibitor, Exemestane

Irina Teslenko, Christy J.W. Watson, Zuping Xia, Gang Chen, Philip Lazarus

Department of Pharmaceutical Sciences, College of Pharmacy and Pharmaceutical Sciences, Washington State University, Spokane, WA 99202

Correspondence to Philip Lazarus, PhD Department of Pharmaceutical Sciences, College of Pharmacy and Pharmaceutical Sciences, Washington State University, 412 E. Spokane Falls Blvd., Spokane, WA 99202-2131; Email: phil.lazarus@wsu.edu

DMD Fast Forward. Published on September 30, 2021 as DOI: 10.1124/dmd.121.000635
This article has not been copyedited and formatted. The final version may differ from this version.

Running Title: Characterization of GSTs in exemestane metabolism

Corresponding author: Philip Lazarus, Department of Pharmaceutical Sciences, College of Pharmacy and Pharmaceutical Sciences, Washington State University, PBS Building Room 431, P.O. Box 1495, Spokane, WA 99202. E-mail: phil.lazarus@wsu.edu

Number of text pages:

Number of tables: 2

Number of figures: 5

Number of supplemental figures: 3

Number of references: 55

Number of words:

Abstract: 250 words

Introduction: 699 words

Discussion: 1,494 words

Abbreviations: Glutathione-S-transferase, GST; exemestane, EXE; 17β-dihydroexemestane, 17β-DHE; selective estrogen modulators, SERM; aromatase inhibitor, AI; tamoxifen, TAM; cytochrome P450, CYP; aldoketoreductase, AKRs; and

DMD Fast Forward. Published on September 30, 2021 as DOI: 10.1124/dmd.121.000635
This article has not been copyedited and formatted. The final version may differ from this version.

carbonyl reductase, CBR; UDP-glucuronosyltransferase, UGT; cysteine, cys; glutathione, GSH; 1-chloro-2,4-dinitrobenzene, CDNB; human liver cytosol, HLC; ultra-pressure liquid chromatography-mass spectrometry, UPLC/MS.

DMD Fast Forward. Published on September 30, 2021 as DOI: 10.1124/dmd.121.000635
This article has not been copyedited and formatted. The final version may differ from this version.

Abstract

Exemestane (EXE) is a hormonal therapy used to treat estrogen receptor positive (ER+) breast cancer by inhibiting the final step of estrogen biosynthesis catalyzed by the enzyme aromatase. Cysteine conjugates of EXE and its active metabolite 17β-dihydro-EXE (17β-DHE) are the major metabolites found in both the urine and plasma of patients taking EXE. The initial step in cysteine conjugate formation is glutathione conjugation catalyzed by the glutathione-S-transferase (GST) family of enzymes. The goal of the present study was to identify cytosolic hepatic GSTs active in the GST-mediated metabolism of EXE and 17β-DHE. Twelve recombinant cytosolic hepatic GSTs were screened for their activity against EXE and 17β-DHE, with glutathionylated EXE and 17β-DHE conjugates detected by ultra-performance liquid chromatography-tandem mass spectrometry. GSTA1, GSTM3 and GSTM1 were active against EXE while only GSTA1 exhibited activity against 17β-DHE. GSTM1 exhibited the highest affinity against EXE with a K_M value that was 3.8- and 7.1-fold lower than that observed for GSTA1 and GSTM3, respectively. Of the three GSTs, GSTM3 exhibited the highest intrinsic clearance against EXE (Cl_{INT}=0.14 nl·min^{-1}·mg^{-1}). The K_M values observed for human liver cytosol against EXE (46 μM) and 17β-DHE (77 μM) were similar to that observed for recombinant GSTA1 (53 μM and 30 μM, respectively). Western blot analysis revealed that GSTA1 and GSTM1 comprised 4.3% and 0.57%, respectively, of total protein in human liver cytosol; GSTM3 was not detected. These data suggest that GSTA1 is the major hepatic cytosolic enzyme involved in the clearance of EXE and its major active metabolite, 17β-DHE.

DMD Fast Forward. Published on September 30, 2021 as DOI: 10.1124/dmd.121.000635
This article has not been copyedited and formatted. The final version may differ from this version.

Significance Statement

Most previous studies related to the metabolism of the aromatase inhibitor, exemestane (EXE), have focused mainly on phase I metabolic pathways as well as the glucuronidation phase II metabolic pathway. However, recent studies have indicated that glutathionylation is the major metabolic pathway for EXE. The present study is the first to characterize hepatic GST activity against EXE and 17β-DHE and to identify GSTA1 and GSTM1 as the major cytosolic GSTs involved in the hepatic metabolism of EXE.

DMD Fast Forward. Published on September 30, 2021 as DOI: 10.1124/dmd.121.000635
This article has not been copyedited and formatted. The final version may differ from this version.

Introduction

Breast cancer is the most commonly diagnosed cancer in women and, despite an overall improvement in breast cancer therapy, continues to be their second leading cause of death (American Cancer Society, 2021). Greater than 75% of diagnosed breast cancers are found to be expressing estrogen receptors (ER), with estrogen contributing to tumor growth and proliferation (Howlader et al., 1975-2013; Osborne and Schiff, 2011). Hormone therapy is most commonly prescribed for early-stage ER-positive breast cancer in post-menopausal women, including treatments with selective estrogen modulators (SERM) or aromatase inhibitors (AI) (Untch and Thomssen, 2010; Early Breast Cancer Trialists' Collaborative, 2015). The mechanism of action of SERMs, including tamoxifen (TAM), is manifested through blocking the ER to prevent the binding of estrogen while AIs including exemestane (EXE) act through suicide inhibition of the enzyme aromatase, disrupting androgen conversion to estrogen in the final step of estrogen biosynthesis (Miller, 1999; Campos, 2004; Eisen et al., 2008; Patel and Bihani, 2018). When compared to tamoxifen, EXE demonstrates a higher clinical efficacy and safety profile (Kieback et al., 2010; Goss et al., 2011). Moreover, long-term use of EXE demonstrated a 65% reduction in the incidence of invasive breast cancer among high-risk but healthy post-menopausal women (Goss et al., 2011). In addition, unlike that observed for TAM, EXE has not been associated with higher risk for thromboembolism or gynecological events such as endometrial cancers, polyps and fibroids. (Coombes et al., 2007; Goss et al., 2011). However, while EXE demonstrates improved treatment efficacy as compared to TAM, the overall response rate of 46% is still relatively low

DMD Fast Forward. Published on September 30, 2021 as DOI: 10.1124/dmd.121.000635
This article has not been copyedited and formatted. The final version may differ from this version.

(Paridaens et al., 2003; Paridaens et al., 2008). In addition, compared to TAM, EXE has been associated with a higher incidence of hot flashes, musculoskeletal pain, and lower bone mineral density (BMD) (Coombes et al., 2007).

EXE is extensively metabolized in patients, with <1% and <10% remaining as unmetabolized EXE in urine and plasma, respectively (Pfizer, 2018). A major route of EXE metabolism is the formation of 17β-dihydroexemestane (17β-DHE), an active metabolite catalyzed by cytochrome P450s (CYPs), aldoketoreductases (AKRs), and carbonyl reductases (CBRs) (Kamdem et al., 2011; Platt et al., 2016; Peterson et al., 2017). 17β-DHE is further conjugated through the glucuronidation pathway to form the inactive 17β-DHE-glucuronide (17β-DHE-Gluc) by UDP-glucuronosyltransferase (UGT) 2B17 (Sun et al., 2010; Luo et al., 2017).

Recently, two novel cysteine (cys) conjugates of EXE and 17β-DHE were identified: 6α-EXE-cys and 6α-17β-DHE-cys, which combined comprised 77% and 35% of the total urinary and plasma EXE metabolites, respectively, in subjects taking EXE (Luo et al., 2018). Cysteine conjugates are formed through a three-step metabolic pathway where the first step involves conjugation with the tripeptide, glutathione (GSH; γ-glu-cys-gly), catalyzed by the glutathione-S-transferase family of enzymes (GSTs) (Hinchman and Ballatori, 1994; Hayes et al., 2005). The glutathione conjugates are subsequently metabolized by γ-glutamyl transferase to remove the glutamyl moiety and dipeptidase to remove the glycyl moiety, ultimately forming the cysteine conjugate which is rapidly excreted. As the first step in this conjugation pathway, GST-mediated glutathionylation is likely a key step in EXE and 17β-DHE metabolism and excretion (Luo et al., 2018; Hanna and Anders, 2019). The ultimate cysteine conjugates render

DMD Fast Forward. Published on September 30, 2021 as DOI: 10.1124/dmd.121.000635
This article has not been copyedited and formatted. The final version may differ from this version.

EXE and DHE more water soluble and more easily excreted; while it is assumed that these conjugates also render EXE and DHE less active, this has not as yet been directly tested.

GSTs are a multifunctional superfamily of enzymes involved in both catalytic and signaling processes. Cytosolic GSTs comprise the largest sub-family of GSTs and are traditionally recognized as the major GSTs involved in phase II metabolism (Habig et al., 1974b; Hayes et al., 2005; Jancova et al., 2010). They are largely expressed in human liver and detoxify a variety of endogenous compounds and exogenous xenobiotics, including environmental pollutants and carcinogens, and many drugs and chemotherapeutic agents (Dostalek and Stark, 2012; Hanna and Anders, 2019). GSTs are also highly polymorphic and been associated with an increased risk for variety of cancers, as well as variability in drug toxicity, cancer resistance, and altered drug metabolism (Perera et al., 2002; Elhasid et al., 2010; Josephy, 2010; Allocati et al., 2018). The goal of the present study was to identify the hepatic cytosolic GSTs important in the metabolism of EXE and 17β-DHE.

DMD Fast Forward. Published on September 30, 2021 as DOI: 10.1124/dmd.121.000635
This article has not been copyedited and formatted. The final version may differ from this version.

Materials and Methods

Chemicals and materials. EXE and 1-chloro-2,4-dinitrobenzene (CDNB) was purchased from Sigma-Aldrich (St Louis, Missouri, USA) while 17β-OH-EXE-d3 (D_3-17β-DHE) and EXE-19-d3 (D_3-EXE) were purchased from Toronto Research Chemicals (North York, ON, Canada). L-Glutathione (reduced) was obtained from Alfa Aesar (Haverhill, MA, USA). Oasis HLB cartridges (1 cc) were purchased from Waters (Milford, MA, USA). Liquid chromatography-mass spectrometry (LC-MS) grade formic acid and acetonitrile were obtained from Thermo-Fisher Scientific (Waltham, MA, USA), and LCMS grade ammonium formate was purchased from Sigma-Aldrich (St Louis, Missouri, USA). Hexane, diethyl ether, potassium hydroxide and methanol were purchased from VWR (Radnor, PA, USA) at ACS quality or higher. Milli-Q water was used for the preparation of all solutions.

Pooled human liver cytosol (HLC; 50 subjects) was purchased from Xenotech (Kansas City, KS, USA). Recombinant human GSTA1, GSTA4, GSTK1, GSTM2, GSTM4 were obtained from Prospec Protein Specialists (East Brunswick, NJ, USA), GSTM1 and GSTM3 were purchased from Novus Bio (Centennial, CO, USA), and GSTA2 was purchased from Sigma-Aldrich (St Louis, Missouri, USA); all purchased recombinant GSTs were >80% pure as indicated by the manufacturer. Luria Broth was purchased from Invitrogen (Carlsbad, California, USA) while isopropyl-1-thio-β-D-galactopyranoside (IPTG) and ampicillin were purchased from Sigma-Aldrich. B-PER complete protein extraction reagent, Ni-NTA affinity purification columns, dextran desalting columns, Pierce BCA protein assay kits, Pierce silver staining kits,

DMD Fast Forward. Published on September 30, 2021 as DOI: 10.1124/dmd.121.000635
This article has not been copyedited and formatted. The final version may differ from this version.

SuperSignal West Pico Plus Chemiluminescent Substrate, and BL21 (DE3) and BL21 (DE3)pLysS competent *E. coli* were purchased from Thermo-Fisher Scientific (Waltham, MA, USA). Monoclonal GSTA1, GSTM1 and polyclonal GSTM3 antibody (mouse Ig) were obtained from Novus Bio (Centennial, CO, USA), while goat anti-mouse IgG secondary antibody (HRP) was purchased from Sigma-Aldrich. All other chemicals were purchased from Thermo-Fisher Scientific unless otherwise specified.

Synthesis of EXE and DHE. EXE and 17β-DHE were synthesized as previously described (Platt et al., 2016). The NMR spectra of the two compounds was recorded on a Bruker Avance I instrument with 500 MHz for proton and 125 MHz for carbon. Chemical shifts were measured based on the residual protium in the NMR deuterium solvent. High resolution mass spectrum (HRMS) was acquired using a Xevo G2-S QToF mass spectrometer (Waters) with a positive electrospray ionization (ESI). The chemical purity was determined on an Acquity H Class UPLC (Waters) with a ACQUITY UPLC BEH C18 column (2.1 x 100 mm; Waters) monitored at 254 nm using a PDA detector.

Synthesis of S-(androsta-1,4-diene-3,17-dion-6α-ylmethyl)-L-glutathione (EXE-GS). EXE (11.7 mg, 0.039 mmol) and L-glutathione (33.4 mg, 0.109 mmol) were added to a 10 mL round-bottom flask under the protection of argon, followed by addition of degassed 1.25 N potassium hydroxide (1 mL). The mixture was stirred at 4^{o}C for 24 h. Water (10 mL) was added to the reaction mixture, which was then washed with dichloromethane (3 x 8 mL). The pH of the water phase was adjusted to ~3 with 2 N HCl,

DMD Fast Forward. Published on September 30, 2021 as DOI: 10.1124/dmd.121.000635
This article has not been copyedited and formatted. The final version may differ from this version.

and it was then stored in a refrigerator overnight. The aqueous sample was loaded onto conditioned Oasis HLB 1 cc cartridges (14 aliquots) followed by sequential elution with water (1.5 mL) and methanol (1.5 mL). The collected methanol solutions were combined, concentrated, and dried to afford EXE-GS (10.6 mg, Y = 45%) as a white solid. ^{1}H NMR (D_2O) δ 7.33 (d, J = 10.1 Hz, 1 H), 6.19 (dd, J_1 = 10.1, J_2 = 1.8 Hz, 1 H), 6.00 (bs, 1 H), 4.50 (dd, J1 = 8.8 Hz, J2 = 5.1 Hz, 1 H), 3.83 (s, 2 H), 3.69 (dd, $J_1 = J_2$ = 6.4 Hz, 1 H), 3.23 (s, 1 H), 3.00 (dd, J_1 = 14.2 Hz, J_2 = 5.1 Hz, 1 H), 2.87 (dd, J_1 = 12.8 Hz, J_2 = 6.3 Hz, 1 H), 2.81 (dd, J_1 = 14.2 Hz, J_2 = 8.8 Hz, 1 H), 2.69 (m, 1 H), 2.60 (dd, J_1 = 12.8 Hz, J_2 = 6.9 Hz, 1 H), 2.45 (m, 3 H), 2.16-2.20 (m, 1 H), 2.00-2.09 (m, 3 H), 2.18-2.20 (m, 2 H), 1.54-1.75 (m, 4 H), 1.07-1.26 (m, 2 H), 1.19 (s, 3 H), 0.90-0.94 (m 1 H), 0.86 (s, 3 H), 0.74 (dd, J_1 = 24.4 Hz, J_2 = 12.3 Hz, 1 H). ^{13}C NMR (D_2O) δ 228.1, 188.9, 174.8, 174.7, 173.8, 173.6, 172.5, 161.5, 125.2, 120.1, 53.8, 53.4, 53.2, 49.6, 48.8, 48.4, 45.0, 41.7, 39.3, 38.5, 35.7, 34.3, 33.8, 31.3, 30.6, 26.1, 22.0, 21.4, 17.7, 13.2. HRMS (ESI) m/z calcd $C_{30}H_{42}N_3O_8S$ $[MH]^+$ 604.2687; found 604.2693; purity >95%.

Synthesis of S-(androsta-1,4-diene-17β-ol-3-on-6α-ylmethyl)-L-gutathione (DHE-GS). DHE-GS was synthesized as described above for EXE-GS using 17β-DHE (10.6 mg, 0.036 mmol) and L-glutathione (37.3 mg, 0.12 mmol) as the starting materials. DHE-GS (2.5 mg, Y = 11%) was purified as a white solid. ^{1}H NMR (D_2O) δ 7.35 (d, J = 10.2 Hz, 1 H), 6.20 (d, J = 10.2 Hz, 1 H), 5.99 (s, 1 H), 4.49 (dd, J_1 = 8.8 Hz, J_2 = 5.2 Hz, 1 H), 3.81 (S, 2 H), 3.68 (dd, $J_1 = J_2$ = 6.4 Hz, 1 H), 3.49 ($J_1 = J_2$ = 8.5 Hz, 1 H), 2.99 (dd, J_1 = 14.1 Hz, J_2 = 5.0 Hz, 1 H), 2.78-2.88 (m, 2 H), 2.55-2.68 (m, 2 H), 2.44 (m, 2 H), 2.06 (m, 3 H), 1.89 (m, 1 H), 1.62-1.77 (m, 4 H), 1.21-1.49 (m, 3 H), 1.18 (s, 3 H), 0.74-

DMD Fast Forward. Published on September 30, 2021 as DOI: 10.1124/dmd.121.000635
This article has not been copyedited and formatted. The final version may differ from this version.

0.96 (m, 3 H), 0.69 (s, 3 H), 0.61 (dd, J_1 = 24.4, J_2 = 12.2, 1 H); ^{13}C NMR (D_2O) δ 188.9, 175.5, 174.7, 174.0, 173.6, 172.4, 162.0, 125.1, 119.9, 81.1, 53.9, 53.8, 53.2, 49.4, 45.2, 42.7, 41.9, 39.5, 39.4, 35.9, 34.8, 33.9, 33.8, 31.3, 28.7, 26.1, 22.9, 22.4, 17.8, 10.6. HRMS (ESI) m/z calcd $C_{30}H_{44}N_3O_8S$ $[MH]^+$ 606.2844, found 606.2900; purity = 94%.

Biosynthesis of D_3-EXE-GS and D_3-17β-DHE-GS. D_3-EXE-GS and D_3-17β-DHE-GS, internal standards for LC-MS analysis of glutathione conjugates of EXE and 17β-DHE were generated in an enzymatic reaction containing pooled HLC (200 µg), 100 mM potassium phosphate (KH_2PO_4) at pH 7.4, and 100 ppm D_3-EXE or 100 ppm D_3-17β-DHE in a total volume of 200 µL. The reaction was incubated at 37°C for 3 min before the addition of 5 mM GSH (Lash et al., 1999; Zarth et al., 2015; Shi et al., 2016). Final mixtures were incubated for 2 h at 37°C and stopped with 200 µL cold acetonitrile. Mixtures were subsequently centrifuged at 16,100 × g for 10 min at 4°C. Supernatants were collected and aliquots of 50 µL were injected onto the ACQUITY UPLC BEH C18 column (2.1 x 100 mm; Waters). The UPLC conditions used were as described below. Fractions containing EXE-GS conjugates were collected at UPLC retention times of 1.2 to 2 min while DHE-GS conjugates were collected at 0.8 min to 1.8 min.

Recombinant Protein Production. The Human Protein Atlas was queried (April 19, 2018) and twelve cytosolic human GSTs were identified to be hepatically expressed: GSTA1, GSTA2, GSTA4, GSTK1, GSTM1, GSTM2, GSTM3, GSTM4, GSTO1, GSTP1, GSTZ1, and GSTT1. GSTA1, GSTA4, GSTK1, GSTM2, GSTM4, GSTM1, GSTM3, and

DMD Fast Forward. Published on September 30, 2021 as DOI: 10.1124/dmd.121.000635
This article has not been copyedited and formatted. The final version may differ from this version.

GSTA2 were purchased commercially; GSTT1, GSTP1, GSTZ1, GSTO1 were not found to be commercially available and were cloned and expressed as described below.

In addition to the non-commercially available GSTs (GSTT1, GSTP1, GSTZ1, and GSTO1), the GSTs that exhibited initial activity against EXE and/or 17β-DHE (GSTA1, GSTM1 and GSTM3) were also cloned and expressed as codon-optimized, recombinant proteins. All GSTs were cloned with a C-terminal histidine (His)-tag. Codon-optimized plasmids encoding wild-type human GSTA1, GSTM3, GSTT1, GSTZ1, GSTP1, and GSTO1 were commercially synthesized by GenScript (Piscataway, NJ, USA) in the pET-15b vector and transformed into chemically competent BL21 (DE3) *E. coli*. GSTM1 codon optimized plasmid was similarly commercially cloned into the pET-15b vector but was transformed into BL21 (DE3)pLysS *E. coli*. Transformed *E. coli* cells were grown under ampicillin selection and the DNA sequence of cloned genes were confirmed with Sanger sequencing (Genewiz, South Plainfield, NJ). Selected bacterial colonies were grown overnight in 10 ml of Luria broth (LB) supplemented with 100 µg/ml of ampicillin at 37°C in a tabletop shaker (250 rpm). A total of 90 ml of fresh LB medium containing 100 µg/ml of ampicillin was inoculated with the overnight culture and grown an additional 2.5 h to reach an optical density (OD) value of 600. The expression of GST protein was induced by the addition of IPTG to a final concentration of 0.5 mM. After induction, cells were grown for an additional 4 h at 37°C and then harvested by centrifugation. The cytosolic fraction was collected following cell lysis with 150 µL Complete Bacterial Protein Extraction Reagent (B-PER) and centrifugation per the manufacturer's protocols.

DMD Fast Forward. Published on September 30, 2021 as DOI: 10.1124/dmd.121.000635
This article has not been copyedited and formatted. The final version may differ from this version.

His-tagged GST proteins were purified from the cytosol by nickel affinity chromatography. Ni-NTA resin spin columns were equilibrated with binding buffer containing 50 mM sodium phosphate, 300 mM NaCl (pH 8.0) and 10 mM imidazole. Each cytosolic lysate was mixed with an equal volume of binding buffer, loaded onto the column, and incubated for 20 min at 4°C for maximal binding. After incubation, the columns were centrifuged at 700 x g for 2 min and the flow through was discarded. Columns were subsequently washed with 20, 60, and 100 mM of imidazole in PBS (pH 7.4), and each of the elutions were collected; GSTP1 His-tagged protein was washed with 20, 60, 100, 150 and 200 mM of imidazole. Using dextran desalting columns, the imidazole was removed, and purified proteins were subsequently stored in PBS (pH 7.4) buffer. A total of 125 ng of protein for each fraction was loaded onto 15% SDS-PAGE gel and all were found to be greater than 90% pure by silver staining (Supplemental Figure 1). As performed for commercially purchased recombinant GST proteins, the activity of purified recombinant proteins was verified using the CDNB assay described below. Pure recombinant enzymes were stored in 200 μL aliquots in 25% glycerol at -20°C.

GST activity assays. The enzymatic activities of recombinant GSTs were verified using a spectrophotometric assay against CDNB, a known substrate for all cytosolic GSTs (Habig et al., 1974a). Reactions were performed using 1 mM CDNB and 1 mM GSH in 100 mM sodium phosphate buffer at 30°C for 6 min. The absorbance of the CDNB-glutathione conjugate product was read at 340 nm (Habig et al., 1974b).

DMD Fast Forward. Published on September 30, 2021 as DOI: 10.1124/dmd.121.000635
This article has not been copyedited and formatted. The final version may differ from this version.

To screen for conjugation activity against EXE and 17β-DHE, activity screens were performed for the eight commercially purchased GSTs (GSTA1, GSTA4, GSTK1, GSTM2, GSTM4, GSTM1, GSTM3, and GSTA2) and the four non-commercially available GSTs that were cloned as recombinant proteins in our lab (GSTT1, GSTP1, GSTO1, GSTZ1). GST recombinant protein (2.5 ng/µl) was mixed with 250 µM of EXE or 17β-DHE in a 25 µL reaction containing 100 mM potassium phosphate. The reaction was pre-incubated at 37°C for 3 min prior to the addition of 5 mM GSH to start the incubation (1 h, 37°C). Incubations were terminated by adding an aliquot (2.5 µL) to ice-cold acetonitrile (5 µL) spiked with 2.5 µL of D_3-EXE-GS or D_3-17β-DHE-GS internal standard. After vortexing and centrifugation at 16,100×g for 10 min at 4°C, supernatants (10 µL) were transferred to a glass sample vial containing 10 µL water. Reactions containing HLC were performed as a positive control, and reactions without enzyme were performed as a negative control.

For enzyme kinetic analysis, EXE-GS formation was examined as described above in reactions incubated for 1 h at 37°C using 2.5-8.0 ng/µL of purified recombinant GSTA1, GSTM1 or GSTM3 protein and varying concentration of EXE (2-250 µM). Similar kinetic assays were also performed with pooled HLC (1 µg/µL). 17β-DHE-GS conjugate formation was examined using recombinant GSTA1 (5 ng/µL) or pooled HLC protein (2 µg/µL) as described above for EXE using 17β-DHE (2-250 µM) as the substrate. Reaction mixtures were processed as described above and loaded onto the ultra-pressure liquid chromatography-mass spectrometry (UPLC/MS) to monitor GS conjugate formation. EXE-GS and 17β-DHE-GS concentrations were quantified using a

DMD Fast Forward. Published on September 30, 2021 as DOI: 10.1124/dmd.121.000635
This article has not been copyedited and formatted. The final version may differ from this version.

standard curve generated from a serial dilution of known amounts of chemically synthesized EXE-GS or 17β-DHE-GS (synthesis described above).

UPLC-MS analysis of GS conjugates. EXE-GS and 17β-DHE-GS conjugate formation was monitored in individual reactions using an UPLC-MS system (Waters) consisting of an Acquity UPLC, an Acquity UPLC BEH C18 column (2.1 x 100 mm), and a XEVO G2-S QToF mass spectrometer. The UPLC flow rate was 0.4 mL/min with a column temperature of 35°C. UPLC conditions for EXE-GS separation were as follows: 0.5 min at 25%:75% of mobile phase B (100% acetonitrile): mobile phase A (5 mM ammonium formate and 0.01% formic acid), a linear gradient to 100% B in 4 min, 1.5 min at 100% B, followed by re-equilibrium with 25% B for 2 min. The UPLC conditions for DHE-GS separation were 2 min at 20% mobile phase B, a linear gradient to 100% B in 4 min, 1.5 min at 100% B, followed by re-equilibrium with 20% B for 2 min. The Waters XEVO G2-S QToF MS was operated in MS/MS mode, and the ESI probe operated in the positive-ion mode with a capillary voltage at 0.6 kV. Nitrogen was used as both the cone and desolvation gases with flow rates maintained at 50 and 800 L/h, respectively. The collision energy for EXE-GS and DHE-GS detection was optimized at 25V with a cone voltage of 30V. Glutathione conjugate formation was detected using the following mass transitions m/z 604.2692→297.184, 607.281→300.203, 606.2849→299.2, 609.3037→302.203 to monitor EXE-GS, D_3-EXE-GS, 17β-DHE-GS and D_3-17β-DHE-GS respectively.

DMD Fast Forward. Published on September 30, 2021 as DOI: 10.1124/dmd.121.000635
This article has not been copyedited and formatted. The final version may differ from this version.

Recombinant GSTA1, GSTM1 and GSTM3 quantification in HLC. Western blot analysis was performed to quantify the amount of GSTA1, GSTM1 and GSTM3 protein present in commercial pooled HLC. Serial dilutions of HLC (25 - 6.25 µg of total protein) and purified recombinant protein (GSTA1 = 1 - 0.125 µg, GSTM1 = 0.25 - 0.03 µg, or GSTM3 = 1 - 0.03 µg) were loaded on three separate 15% SDS-polyacrylamide gels, and after electrophoresis were transferred to PVDF membranes using an iBlot system (Thermo Fisher Scientific). The membranes were blocked overnight at 4˚C in blocking buffer (5% nonfat dry milk in Tris-buffered saline containing 50mM Tris-Cl, pH 7.6; 0.9% NaCl, 0.1% Tween 20 (TBST)), and subsequently washed 3X times (10 min each) with TBST. For GSTA1, GSTM1 and GSTM3, membranes were probed with mouse monoclonal GSTA1 antibody (1:400 dilution), mouse monoclonal GSTM1 antibody (1:1,000 dilution) and mouse polyclonal GSTM3 antibody (1:250), respectively, for 2 h in blocking buffer followed by a goat anti-mouse secondary antibody (1:10,000 dilution) in blocking buffer for 1 h. Bands on the membranes probed with anti-GSTM1 and anti-GSTA1 were visualized with the Novex ECL Chemiluminescent Kit, while the membrane probed with anti-GSTM3 was visualized with SuperSignal Femto Maximum Sensitivity Substrate. The densitometry analysis of images at 400 sec exposure time were performed using Image J software (https://imagej.nih.gov/ij/; National Institutes of Health, Bethesda, MD). Western blot experiments were performed in triplicate.

Enzyme kinetic analysis. Kinetic parameters were determined utilizing the Michaelis-Menten equation using GraphPad Prism software (version 6.01). V_{max} values

DMD Fast Forward. Published on September 30, 2021 as DOI: 10.1124/dmd.121.000635
This article has not been copyedited and formatted. The final version may differ from this version.

were calculated as nmol/min/mg of pure recombinant protein. All reported values were results of three independent experiments.

DMD Fast Forward. Published on September 30, 2021 as DOI: 10.1124/dmd.121.000635
This article has not been copyedited and formatted. The final version may differ from this version.

Results

*Identification of EXE-GS and DHE-GS conjugates***.** Chemically synthesized standard EXE-GS (S-(androsta-1,4-diene-3,17-dion-6α-ylmethyl)-L-glutathione) and 17β-DHE-GS (S-(androsta-1,4-diene-17β-ol-3-on-6α-ylmethyl)-L-gutathione) at 10 ppm were used to confirm the identity of EXE-GS and 17β-DHE-GS conjugates in the screening assays. As shown by representative chromatograms in Figure 1, panel A depicts the EXE-GS standard, with one major UV peak (254 nm) at 1.2 min and a corresponding parent ion spectrum with an $(m/z)^+$ of 604.27, which matches with the predicted [EXE-GS+H^+] ion ($C_{30}H_{42}N_3O_8S$) $(m/z)^+$ = 604.28. The chemical structure of the synthesized EXE-GS was confirmed by NMR (described in the Materials and Methods above) and found to be 95% pure. A representative UV chromatogram of a glutathione conjugation assay utilizing HLC and EXE as a substrate (panel B) shows the EXE-GS parent ion of $(m/z)^+$ = 604.28 at 1.2 min. A comparable UV trace of the 17β-DHE-GS standard is shown in Panel D with the main peak detected by UV at 0.80 min and the corresponding parent ion $(m/z)^+$ = 606.28 matching with the predicted [17β-DHE-GS+H^+] ion ($C_{30}H_{44}N_3O_8S$) [$(m/z)^+$ = 606.28]. The synthesized 17β-DHE-GS standard was also confirmed by NMR with estimated purity of 94%. Panel E shows glutathione conjugate formation in HLC with 17β-DHE as the substrate. The peak at 0.90 min in panel E has an $(m/z)^+$ = 606.28, and matched with synthesized standard in panel D, confirming the identity of the peak as glutathione conjugate of 17β-DHE.

A total of 12 recombinant hepatic cytosolic GSTs (GSTA1, GSTA2, GSTA4, GSTK1, GSTM1, GSTM2, GSTM3, GSTM4, GSTO1, GSTP1, GSTZ1, and GSTT1)

DMD Fast Forward. Published on September 30, 2021 as DOI: 10.1124/dmd.121.000635
This article has not been copyedited and formatted. The final version may differ from this version.

were screened for activity against EXE and its active metabolite 17β-DHE. All 12 GSTs were active against the universal GST substrate, CDNB (Supplemental Figure 2). A sensitive MS/MS method (described above) was developed to detect glutathione conjugates of EXE and 17β-DHE. As shown in Figure 2, GSTA1, GSTM1, and GSTM3 exhibited significant activity against EXE in screening assays (panel A), with GSTA1 > GSTM3 ~ GSTM1. None of the other recombinant cytosolic GST enzymes tested (GSTA2, GSTA4, GSTK1, GSTM2, GSTM4, GSTO1, GSTP1, GSTZ1 and GSTT1) exhibited activity against EXE. Interestingly, only GSTA1 exhibited activity against 17β-DHE among the 12 cytosolic GSTs tested (panel B).

Representative Michaelis-Menten plots of EXE-GS and 17β-DHE-GS formation are shown in Figure 3. Kinetic analysis of EXE-GS formation by recombinant GSTA1, GSTM1 and GSTM3 enzymes demonstrated that GSTM1 exhibited the highest affinity for EXE (K_M = 14 ± 4.1 μM) followed by GSTA1 (K_M = 53 ± 17 μM) and GSTM3 (K_M = 99 ± 6.0 μM; Table 1). The apparent K_M (46 ± 12 μM) for EXE-GS formation in HLC was similar to that observed for GSTA1. GSTM3 exhibited the highest rate of EXE-GS formation (V_{max} = 14 ± 1.4 nmol·min^{-1}·mg^{-1}) which was approximately 3- and 32-fold higher than that observed for GSTA1 (V_{max} = 4.7 ± 2.9 nmol·min^{-1}·mg^{-1}) and GSTM1 (V_{max} = 0.43 ± 0.29 nmol·min^{-1}·mg^{-1}), respectively. Overall, recombinant GSTM3 exhibited a marginally higher intrinsic clearance of EXE (CL_{INT} = 0.14 ± 0.092 nl·min^{-1}·mg^{-1}) as compared to GSTA1 (CL_{INT} = 0.085 ± 0.043 nl·min^{-1}·mg^{-1}) but exhibited a CL_{INT} that was 4.4-fold higher than that observed for GSTM1 (CL_{INT} = 0.032 ± 0.017 nl·min^{-1}·mg^{-1}).

DMD Fast Forward. Published on September 30, 2021 as DOI: 10.1124/dmd.121.000635
This article has not been copyedited and formatted. The final version may differ from this version.

Relative expression of GSTA1, GSTM1 and GSTM3 in pooled HLC. Quantitative Western blot analysis was performed to determine the relative amounts of each active GST present in pooled HLC. Commercial antibodies for GSTA1, GSTM1 and GSTM3 were first verified for specificity and cross reactivity (Supplemental Figure 3). Western blot containing serial dilutions of HLC and purified recombinant GSTA1, GSTM1 and GSTM3 proteins were then probed with each specific antibody (representative images shown in Figure 4). Densitometry analysis of three independent experiments each containing pure recombinant protein as a standard estimated that GSTA1 and GSTM1 comprised 0.043 ± 0.0051 and 0.0057 ± 0.00043 µg of GST per µg of HLC, respectively (Table 2). No GSTM3 protein were detected in HLC by Western blot analysis.

DMD Fast Forward. Published on September 30, 2021 as DOI: 10.1124/dmd.121.000635
This article has not been copyedited and formatted. The final version may differ from this version.

Discussion

Glutathionylation is an important step in the xenobiotic detoxification pathway of many compounds and might play an important role in the rate of excretion and elimination of EXE, thereby contributing to the variation observed in EXE treatment efficacy and side effects (Jancova et al., 2010). As shown in previous studies, cysteine conjugates of EXE comprise 77% of total urinary metabolites, while in plasma cysteine conjugate levels are similar to another major metabolite,17β-DHE-Gluc (Luo et al., 2018). These data suggest that the formation of cysteine conjugates is a major route of metabolism of EXE. Cysteine conjugates are formed through a three-step pathway similar to that observed in the mercapturic acid synthesis pathway, with the first step, GSH conjugation, catalyzed by the GST family of enzymes (Hanna and Anders, 2019). Glutathione conjugates are typically inactive, less toxic, more water soluble and more readily excreted than parent unconjugated compound (Allocati et al., 2018). Subsequently, the glutamyl moiety is removed by γ-glutamyltransferases (GGT) and the glycyl moiety is removed by dipeptidases, and cysteine conjugates are excreted in the urine (Hanna and Anders, 2019). This three-step pathway has been verified for EXE through *in vitro* biosynthesis, with the resulting enzymatically synthesized cysteine conjugate of EXE matching both chemically synthesized EXE-cys, as well as through *ex vivo* analysis of urinary EXE-cys detected in subjects taking EXE (Luo et al., 2018).

In the present study, we demonstrate that GSTA1, GSTM1, and GSM3 are the major enzymes forming the EXE-GS conjugate and that GSTA1 is the primary GST leading to the formation of 17β-DHE-GS (see Figure 5). The alpha class of GSTs are the major form of the enzyme expressed in hepatocytes and they play a critical role in

DMD Fast Forward. Published on September 30, 2021 as DOI: 10.1124/dmd.121.000635
This article has not been copyedited and formatted. The final version may differ from this version.

cellular defense against oxidative stress by catalyzing glutathione peroxidase reactions (e.g., fatty acid hydroperoxides, phospholipid hydroperoxides) and detoxification of xenobiotics such as environmental carcinogens [e.g., polycyclic aromatic hydrocarbons (PAHs)] and therapeutic drugs (busulfan, cyclophosphamide and chlorambucil) (Czerwinski et al., 1996; Coles and Kadlubar, 2005; Bertholee et al., 2017; Attia et al., 2021). GSTA1 is quickly released into the bloodstream during hepatocellular damage, with serum GSTA1 concentration has been used as a biomarker for hepatic or renal injury (Mikstacki et al., 2016; Li et al., 2017). In addition to being involved in various catalytic processes, GSTA1 was also reported to be a modulator of the c-Jun N-terminal kinase (JNK) signaling pathway by protein-protein interactions. JNK functions as a critical control point in the mitogen-activated protein kinase (MAPK) pathways during cellular stress (Adnan et al., 2012; Pljesa-Ercegovac et al., 2018), suggesting that GSTA1 plays multiple important roles in the cell. GSTA1 is the major GST expressed in liver (Coles and Kadlubar, 2005) and is the only GST that showed activity against both EXE and 17β-DHE. According to the Human Protein Atlas, hepatic GSTA1 mRNA expression is 1,958 protein-coding transcripts per million (pTPM), which is 5.5-fold higher than that observed for GSTM1 (353 pTPM) and 169-fold higher than GSTM3 (12 pTPM) [http://www.proteinatlas.org; queried on July 10th, 2021; (Uhlén et al., 2015)]. Additional sources have suggested that GSTA1 comprises 2-5% of total soluble protein in hepatocytes (Beckett and Hayes, 1993; Hayes and Pulford, 1995). In the present study, Western blot analysis of pooled HLC showed that GSTA1 comprises 4.3% of the total cytosolic protein, a value consistent with these previous reports. The affinities for EXE (K_m = 46 ± 12 μM) and 17β-DHE (K_m = 51 ± 14 μM) in HLC glutathione conjugation

DMD Fast Forward. Published on September 30, 2021 as DOI: 10.1124/dmd.121.000635
This article has not been copyedited and formatted. The final version may differ from this version.

were similar to those observed for purified GSTA1 (K_M = 53 ± 17 μM and 32 ± 12 μM, respectively), supporting a major role for GSTA1 as the major GST active in the metabolism of both EXE and 17β-DHE in human liver.

The rate of GS conjugate formation (i.e., V_{max}) and intrinsic clearance (i.e. CL_{INT}) by recombinant GSTA1 for EXE was 9.7- and 5-fold higher, respectively, than that observed for 17β-DHE-GS. These data are consistent with previous metabolomic studies demonstrating that EXE-cys is the major metabolite observed in the urine of women taking EXE, where the mean levels of EXE-cys in the urine (5.9 ± 0.58 nmol/mg creatinine) and plasma (22 ± 2.9 nM) were 3.3- and 3.7-fold higher, respectively, than that observed for 17β-DHE-cys in these subjects (Luo et al., 2018). 17β-DHE-Gluc, another major metabolite of EXE, is found at comparable levels to EXE-cys in plasma but were 4.2-fold lower in urine in patients taking EXE (Luo et al., 2018). These data further suggest that cysteine conjugate formation through GS conjugation of EXE is the primary route of elimination of EXE via phase II metabolism.

Consistent with other GST isoforms, GSTM1 catalyzes a variety of different electrophilic compounds including carcinogens, environmental toxins, therapeutic drugs [busulfan, acetaminophen, azathioprine, cisplatin, etc. (Czerwinski et al., 1996; Peters et al., 2000; Arakawa et al., 2012) and products of oxidative stress (Marinković et al., 2013). Similar to that observed for GSTA1, GSTM1 is also involved in the MAPK signal transduction pathway through complexes with apoptosis signal-regulating kinase 1 (ASK1) and repression of apoptotic cell death (Cho et al., 2001), supporting its important role in multiple cellular processes. The data from the present study suggests that GSTM1 also plays an important role in the hepatic clearance of EXE. GSTM1

DMD Fast Forward. Published on September 30, 2021 as DOI: 10.1124/dmd.121.000635
This article has not been copyedited and formatted. The final version may differ from this version.

exhibited the highest affinity of any GST enzyme for EXE with a K_M value of 14 µM, which is 3.7-fold lower than GSTA1 (K_M = 53 ± 17 µM). However, GSTM1 comprised only 0.57% of all hepatic cytosolic protein as determined by quantitative Western blot analysis, a level that was >7.5-fold lower than that observed for GSTA1 in the same experiments, suggesting that its role in hepatic EXE metabolism may be secondary to GSTA1.

The third isoform, GSTM3, shows the highest intrinsic clearance values for EXE *in vitro* (0.14 nl·min^{-1}·mg^{-1}) among the three GSTs. However, it likely plays a minimal role in the hepatic clearance of EXE since it was not detected in HLC. These data are consistent with that observed in the Human Protein Atlas database, which showed that GSTM3 mRNA levels are 169-fold less abundant than GSTA1 and 29-fold less abundant than GSTM1 in liver [http://www.proteinatlas.org; queried on July 10th, 2021; (Uhlén et al., 2015)]. GSTM3 might, however, contribute to the first-pass metabolism of EXE since its expression is about 2-fold higher than GSTM1 in the small intestine (http://www.proteinatlas.org; queried on July 10th, 2021).

EXE reduction to 17β-DHE during phase I metabolism and the subsequent glucuronidation of 17β-DHE by UGT2B17 has been extensively studied (Sun et al., 2010; Kamdem et al., 2011; Platt et al., 2016; Peterson et al., 2017). Deletion of UGT2B17 was associated with decreased 17β-DHE-Gluc metabolite levels and increased levels of 17β-DHE (Luo et al., 2017). Recent studies examining the potential correlation between the UGT2B17 deletion and commonly reported side effects (fatigue, hot flashes, and joint pain) in postmenopausal women taking EXE found that the UGT2B17 gene deletion is associated with a higher risk of severe fatigue, hot flashes,

DMD Fast Forward. Published on September 30, 2021 as DOI: 10.1124/dmd.121.000635
This article has not been copyedited and formatted. The final version may differ from this version.

and joint pain (Ho et al., 2020). Interestingly, common functional polymorphisms also exist for several GSTs, including GSTA1 and GSTM1. GSTA1 has 3 linked functional single nucleotide polymorphisms (SNPs) in the promoter region resulting in two allelic variants, GSTA1*A and GSTA1*B, with the GSTA1*B minor allele frequency (MAF) at 0.43-0.49 in the Caucasian population (Mikstacki et al., 2016; Michaud et al., 2019). The promoter SNP in position -52 (G>A) has functional importance since it impairs the binding of the Sp1 transcription factor, reduces promoter activity, and is associated with altered hepatic GSTA1 expression and increased risk for a variety of cancers (Coles et al., 2001; Coles and Kadlubar, 2005) The GSTA1*B genotype was also associated with interindividual variability in busulfan (BU) clearance in children undergoing hematopoietic stem cell transplantation (HSCT) leading to the higher incidence of HSCT related toxicities such as Sinusoidal Obstruction Syndrome (SOS), acute Graft-versus-Host Disease (GvHD) and other treatment-related toxicities (Ansari et al., 2017). In addition, GSTM1 has a whole-gene deletion polymorphism that is highly prevalent (minor allele frequency = 48-57%) in the Caucasian population and has been associated with increased risk for a variety of cancers (Geisler and Olshan, 2001). The GSTM1 null genotype also has been linked with alterations in drug metabolism and clinical efficacy. For example, the GSTM1 null genotype has been associated with lower efficacy in patients taking azathioprine (AZA) as an immunosuppressant during inflammatory bowel disease (Lucafò et al., 2019). These GST functional variants may therefore contribute to the variability in hepatic EXE metabolism in the population.

In conclusion, *in vitro* studies suggest that GSTA1 is the major isoform responsible for the hepatic metabolism of EXE and 17β-DHE. GSTM1 contributes to the

hepatic clearance of EXE, but not 17β-DHE. While GSTM3 is active against EXE, it does not contribute significantly to hepatic clearance given its negligible expression in the liver. Further studies examining the role of functional polymorphisms in GSTA1 and GSTM1 on EXE metabolism should be performed to better evaluate the role of these enzymes on individual differences in EXE efficacy, side effects and overall treatment outcomes.

DMD Fast Forward. Published on September 30, 2021 as DOI: 10.1124/dmd.121.000635
This article has not been copyedited and formatted. The final version may differ from this version.

Conflict of interests

None declared.

Acknowledgements

The authors would like to thank Shaman Luo for her helpful contributions to the study.

Authorship contributions

Participated in research design: Teslenko and Lazarus.

Conducted experiments: Teslenko

Contributed new reagents or analytic tools: Xia

Performed data analysis: Teslenko, Chen, Lazarus.

Wrote or contributed to the writing of the manuscript: Teslenko, Watson, Xia, Chen, and Lazarus.

DMD Fast Forward. Published on September 30, 2021 as DOI: 10.1124/dmd.121.000635
This article has not been copyedited and formatted. The final version may differ from this version.

References

Adnan H, Antenos M, and Kirby GM (2012) The effect of menadione on glutathione S-transferase A1 (GSTA1): c-Jun N-terminal kinase (JNK) complex dissociation in human colonic adenocarcinoma Caco-2 cells. *Toxicology letters* **214:**53-62.

Allocati N, Masulli M, Di Ilio C, and Federici L (2018) Glutathione transferases: substrates, inihibitors and pro-drugs in cancer and neurodegenerative diseases. *Oncogenesis* **7:**8.

American Cancer Society (2021) Cancer Facts & Figures.

Ansari M, Curtis PH, Uppugunduri CRS, Rezgui MA, Nava T, Mlakar V, Lesne L, Théoret Y, Chalandon Y, Dupuis LL, Schechter T, Bartelink IH, Boelens JJ, Bredius R, Dalle JH, Azarnoush S, Sedlacek P, Lewis V, Champagne M, Peters C, Bittencourt H, and Krajinovic M (2017) GSTA1 diplotypes affect busulfan clearance and toxicity in children undergoing allogeneic hematopoietic stem cell transplantation: a multicenter study. *Oncotarget* **8:**90852-90867.

Arakawa S, Maejima T, Fujimoto K, Yamaguchi T, Yagi M, Sugiura T, Atsumi R, and Yamazoe Y (2012) Resistance to acetaminophen-induced hepatotoxicity in glutathione S-transferase Mu 1-null mice. *The Journal of toxicological sciences* **37:**595-605.

Attia DHS, Eissa M, Samy LA, and Khattab RA (2021) Influence of glutathione S transferase A1 gene polymorphism (-69C > T, rs3957356) on intravenous cyclophosphamide efficacy and side effects: a case-control study in Egyptian patients with lupus nephritis. *Clinical rheumatology* **40:**753-762.

Beckett GJ and Hayes JD (1993) Glutathione S-transferases: biomedical applications. *Advances in clinical chemistry* **30:**281-380.

Bertholee D, Maring JG, and van Kuilenburg AB (2017) Genotypes Affecting the Pharmacokinetics of Anticancer Drugs. *Clinical pharmacokinetics* **56:**317-337.

Campos SM (2004) Aromatase inhibitors for breast cancer in postmenopausal women. *Oncologist* **9:**126-136.

Cho SG, Lee YH, Park HS, Ryoo K, Kang KW, Park J, Eom SJ, Kim MJ, Chang TS, Choi SY, Shim J, Kim Y, Dong MS, Lee MJ, Kim SG, Ichijo H, and Choi EJ (2001) Glutathione S-transferase mu modulates the stress-activated signals by suppressing apoptosis signal-regulating kinase 1. *J Biol Chem* **276:**12749-12755.

Coles BF and Kadlubar FF (2005) Human alpha class glutathione S-transferases: genetic polymorphism, expression, and susceptibility to disease. *Methods in enzymology* **401:**9-42.

Coles BF, Morel F, Rauch C, Huber WW, Yang M, Teitel CH, Green B, Lang NP, and Kadlubar FF (2001) Effect of polymorphism in the human glutathione S-transferase A1 promoter on hepatic GSTA1 and GSTA2 expression. *Pharmacogenetics* **11:**663-669.

Coombes RC, Kilburn LS, Snowdon CF, Paridaens R, Coleman RE, Jones SE, Jassem J, Van de Velde CJ, Delozier T, Alvarez I, Del Mastro L, Ortmann O, Diedrich K, Coates AS, Bajetta E, Holmberg SB, Dodwell D, Mickiewicz E, Andersen J, Lonning PE, Cocconi G, Forbes J, Castiglione M, Stuart N, Stewart A, Fallowfield LJ, Bertelli G, Hall E, Bogle RG, Carpentieri M, Colajori E, Subar M, Ireland E, Bliss JM, and Intergroup Exemestane S (2007) Survival and safety of exemestane versus tamoxifen after 2-3 years' tamoxifen treatment (Intergroup Exemestane Study): a randomised controlled trial. *Lancet* **369:**559-570.

Czerwinski M, Gibbs JP, and Slattery JT (1996) Busulfan conjugation by glutathione S-transferases alpha, mu, and pi. *Drug metabolism and disposition: the biological fate of chemicals* **24:**1015-1019.

Dostalek M and Stark A-K (2012) Glutathione S-Transferases, in: *Metabolism of Drugs and Other Xenobiotics*, pp 147-164.

Early Breast Cancer Trialists' Collaborative G (2015) Aromatase inhibitors versus tamoxifen in early breast cancer: patient-level meta-analysis of the randomised trials. *Lancet* **386:**1341-1352.

Eisen A, Trudeau M, Shelley W, Messersmith H, and Pritchard KI (2008) Aromatase inhibitors in adjuvant therapy for hormone receptor positive breast cancer: a systematic review. *Cancer treatment reviews* **34:**157-174.

Elhasid R, Krivoy N, Rowe JM, Sprecher E, Adler L, Elkin H, and Efrati E (2010) Influence of glutathione S-transferase A1, P1, M1, T1 polymorphisms on oral busulfan pharmacokinetics in children with congenital hemoglobinopathies undergoing hematopoietic stem cell transplantation. *Pediatric blood & cancer* **55:**1172-1179.

Geisler SA and Olshan AF (2001) GSTM1, GSTT1, and the risk of squamous cell carcinoma of the head and neck: a mini-HuGE review. *American journal of epidemiology* **154:**95-105.

Goss PE, Ingle JN, Ales-Martinez JE, Cheung AM, Chlebowski RT, Wactawski-Wende J, McTiernan A, Robbins J, Johnson KC, Martin LW, Winquist E, Sarto GE, Garber JE, Fabian CJ, Pujol P, Maunsell E, Farmer P, Gelmon KA, Tu D, Richardson H, and Investigators NCMS (2011) Exemestane for breast-cancer prevention in postmenopausal women. *N Engl J Med* **364:**2381-2391.

Habig WH, Pabst MJ, Fleischner G, Gatmaitan Z, Arias IM, and Jakoby WB (1974a) The identity of glutathione S-transferase B with ligandin, a major binding protein of liver. *Proceedings of the National Academy of Sciences of the United States of America* **71:**3879-3882.

Habig WH, Pabst MJ, and Jakoby WB (1974b) Glutathione S-transferases. The first enzymatic step in mercapturic acid formation. *J Biol Chem* **249:**7130-7139.

Hanna PE and Anders MW (2019) The mercapturic acid pathway. *Crit Rev Toxicol* **49:**819-929.

Hayes JD, Flanagan JU, and Jowsey IR (2005) Glutathione transferases. *Annual review of pharmacology and toxicology* **45:**51-88.

Hayes JD and Pulford DJ (1995) The Glut athione S-Transferase Supergene Family: Regulation of GST and the Contribution of the lsoenzymes to Cancer Chemoprotection and Drug Resistance Part I. *Critical Reviews in Biochemistry and Molecular Biology* **30:**445-520.

Hinchman CA and Ballatori N (1994) Glutathione conjugation and conversion to mercapturic acids can occur as an intrahepatic process. *Journal of toxicology and environmental health* **41:**387-409.

Ho V, Pasquet R, Luo S, Chen G, Goss P, Tu D, Lazarus P, and Richardson H (2020) Variation in the UGT2B17 genotype, exemestane metabolism and menopause-related toxicities in the CCTG MAP.3 trial. *Breast cancer research and treatment* **183:**705-716.

Howlader N, Noone AM, Krapcho M, Miller D, Bishop K, Altekruse SF, Kosary CL, Yu M, Ruhl J, Tatalovich Z, Mariotto A, Lewis DR, Chen HS, Feuer EJ, and Cronin KA (1975-2013) SEER Cancer Statistics Review.

Jancova P, Anzenbacher P, and Anzenbacherova E (2010) Phase II drug metabolizing enzymes. *Biomedical papers of the Medical Faculty of the University Palacky, Olomouc, Czechoslovakia* **154:**103-116.

Josephy PD (2010) Genetic variations in human glutathione transferase enzymes: significance for pharmacology and toxicology. *Human genomics and proteomics : HGP* **2010:**876940.

Kamdem LK, Flockhart DA, and Desta Z (2011) In vitro cytochrome P450-mediated metabolism of exemestane. *Drug metabolism and disposition: the biological fate of chemicals* **39:**98-105.

Kieback DG, Harbeck N, Bauer W, Hadji P, Weyer G, Menschik T, and Hasenburg A (2010) Endometrial effects of exemestane compared to tamoxifen within the Tamoxifen Exemestane Adjuvant Multicenter (TEAM) trial: results of a prospective gynecological ultrasound substudy. *Gynecol Oncol* **119:**500-505.

Lash LH, Lipscomb JC, Putt DA, and Parker JC (1999) Glutathione conjugation of trichloroethylene in human liver and kidney: kinetics and individual variation. *Drug metabolism and disposition: the biological fate of chemicals* **27:**351-359.

Li R, Liu F, Chang Y, Ma X, Li M, Li C, Shi C, He J, Li Y, Li Z, Lin Y, Han Q, Zhao Y, and Wang D (2017) Glutathione S-transferase A1 (GSTA1) as a marker of acetaminophen-induced hepatocyte injury in vitro. *Toxicology mechanisms and methods* **27:**401-407.

Lucafò M, Stocco G, Martelossi S, Favretto D, Franca R, Malusà N, Lora A, Bramuzzo M, Naviglio S, Cecchin E, Toffoli G, Ventura A, and Decorti G (2019) Azathioprine Biotransformation in Young Patients with Inflammatory Bowel Disease: Contribution of Glutathione-S Transferase M1 and A1 Variants. *Genes* **10**.

Luo S, Chen G, Truica C, Baird CC, Leitzel K, and Lazarus P (2017) Role of the UGT2B17 deletion in exemestane pharmacogenetics. *The pharmacogenomics journal*.

Luo S, Chen G, Truica CI, Baird CC, Xia Z, and Lazarus P (2018) Identification and Quantification of Novel Major Metabolites of the Steroidal Aromatase Inhibitor, Exemestane. *Drug metabolism and disposition: the biological fate of chemicals* **46:**1867-1878.

Marinković N, Pasalić D, and Potocki S (2013) Polymorphisms of genes involved in polycyclic aromatic hydrocarbons' biotransformation and atherosclerosis. *Biochemia medica* **23:**255-265.

Michaud V, Tran M, Pronovost B, Bouchard P, Bilodeau S, Alain K, Vadnais B, Franco M, Bélanger F, and Turgeon J (2019) Impact of GSTA1 Polymorphisms on Busulfan Oral Clearance in Adult Patients Undergoing Hematopoietic Stem Cell Transplantation. *Pharmaceutics* **11**.

Mikstacki A, Skrzypczak-Zielinska M, Zakerska-Banaszak O, Tamowicz B, Skibinska M, Molinska-Glura M, Szalata M, and Slomski R (2016) Impact of CYP2E1, GSTA1 and GSTP1 gene variants on serum alpha glutathione S-transferase level in patients undergoing anaesthesia. *BMC medical genetics* **17:**40.

Miller WR (1999) Biology of aromatase inhibitors: pharmacology/endocrinology within the breast. *Endocr Relat Cancer* **6:**187-195.

Osborne CK and Schiff R (2011) Mechanisms of endocrine resistance in breast cancer. *Annu Rev Med* **62:**233-247.

Paridaens R, Dirix L, Lohrisch C, Beex L, Nooij M, Cameron D, Biganzoli L, Cufer T, Duchateau L, Hamilton A, Lobelle JP, Piccart M, European Organization for the R, and Treatment of Cancer - Investigational Drug Branch for Breast C (2003) Mature results of a randomized phase II multicenter study of exemestane versus tamoxifen as first-line hormone therapy for postmenopausal women with metastatic breast cancer. *Ann Oncol* **14:**1391-1398.

Paridaens RJ, Dirix LY, Beex LV, Nooij M, Cameron DA, Cufer T, Piccart MJ, Bogaerts J, and Therasse P (2008) Phase III study comparing exemestane with tamoxifen as first-line hormonal treatment of metastatic breast cancer in postmenopausal women: the European Organisation for Research and Treatment of Cancer Breast Cancer Cooperative Group. *Journal of clinical oncology : official journal of the American Society of Clinical Oncology* **26:**4883-4890.

Patel HK and Bihani T (2018) Selective estrogen receptor modulators (SERMs) and selective estrogen receptor degraders (SERDs) in cancer treatment. *Pharmacol Ther* **186:**1-24.

Perera FP, Mooney LA, Stampfer M, Phillips DH, Bell DA, Rundle A, Cho S, Tsai W-Y, Ma J, Blackwood A, and Tang D (2002) Associations between carcinogen–DNA damage, glutathione S-transferase genotypes, and risk of lung cancer in the prospective Physicians' Health Cohort Study. *Carcinogenesis* **23:**1641-1646.

Peters U, Preisler-Adams S, Hebeisen A, Hahn M, Seifert E, Lanvers C, Heinecke A, Horst J, Jürgens H, and Lamprecht-Dinnesen A (2000) Glutathione S-transferase genetic polymorphisms and individual sensitivity to the ototoxic effect of cisplatin. *Anti-cancer drugs* **11:**639-643.

Peterson A, Xia Z, Chen G, and Lazarus P (2017) In vitro metabolism of exemestane by hepatic cytochrome P450s: impact of nonsynonymous polymorphisms on formation of the active metabolite 17beta-dihydroexemestane. *Pharmacology research & perspectives* **5:**e00314.

Pfizer (2018) Aromasin Exemestane Tablets, http://www.pfizer.com/files/products/uspi_aromasin.pdf.

Platt A, Xia Z, Liu Y, Chen G, and Lazarus P (2016) Impact of nonsynonymous single nucleotide polymorphisms on in-vitro metabolism of exemestane by hepatic cytosolic reductases. *Pharmacogenetics and genomics* **26:**370-380.

Pljesa-Ercegovac M, Savic-Radojevic A, Matic M, Coric V, Djukic T, Radic T, and Simic T (2018) Glutathione Transferases: Potential Targets to Overcome Chemoresistance in Solid Tumors. *International journal of molecular sciences* **19**.

Shi J, Xie C, Liu H, Krausz KW, Bewley CA, Zhang S, Tang L, Zhou Z, and Gonzalez FJ (2016) Metabolism and Bioactivation of Fluorochloridone, a Novel Selective Herbicide, in Vivo and in Vitro. *Environ Sci Technol* **50:**9652-9660.

Sun D, Chen G, Dellinger RW, Sharma AK, and Lazarus P (2010) Characterization of 17-dihydroexemestane glucuronidation: potential role of the UGT2B17 deletion in exemestane pharmacogenetics. *Pharmacogenetics and genomics* **20:**575-585.

Uhlén M, Fagerberg L, Hallström BM, Lindskog C, Oksvold P, Mardinoglu A, Sivertsson Å, Kampf C, Sjöstedt E, Asplund A, Olsson I, Edlund K, Lundberg E, Navani S, Szigyarto CA-K, Odeberg J, Djureinovic D, Takanen JO, Hober S, Alm T, Edqvist P-H, Berling H, Tegel H, Mulder J, Rockberg J, Nilsson P, Schwenk JM, Hamsten M, von Feilitzen K, Forsberg M, Persson L, Johansson F, Zwahlen M, von Heijne G, Nielsen J, and Pontén F (2015) Tissue-based map of the human proteome. *Science* **347:**1260419.

Untch M and Thomssen C (2010) Clinical practice decisions in endocrine therapy. *Cancer Invest* **28 Suppl 1:**4-13.

Zarth AT, Murphy SE, and Hecht SS (2015) Benzene oxide is a substrate for glutathione S-transferases. *Chem Biol Interact* **242:**390-395.

DMD Fast Forward. Published on September 30, 2021 as DOI: 10.1124/dmd.121.000635
This article has not been copyedited and formatted. The final version may differ from this version.

Footnotes

These studies were made possible through the gracious support of the Public Health Service, the National Institutes of Health National Cancer Institute, U.S. Department of Health and Human Services [Grant 1R01-CA164366-01A1, to P Lazarus].

Citation of meeting abstracts

Teslenko, I., Chen, G., Xia, Z., Lazarus, P (2018), Role of glutathione-S-transferases in the metabolism of the anti-cancer agent and aromatase inhibitor, exemestane. The FASEB Journal, 32: S1 (https://doi.org/10.1096/fasebj.2018.32.1_supplement.566.10)

Teslenko, I., Chen, G., Watson, C., Xia, Z., Lazarus, P (2019), Glutathione-S-Transferases Represent a Novel Pathway Contributing to the Metabolic Clearance of the Anti-Cancer Agent and Aromatase Inhibitor, Exemestane. The FASEB Journal, 33: S1 (https://doi.org/10.1096/fasebj.2019.33.1_supplement.508.7)

Teslenko, I., Chen, G., Watson, C., Lazarus, P (2020), Cytosolic glutathione-S-transferase A1 (GSTA1) plays a primary role in the metabolic clearance of the aromatase inhibitor, Exemestane. The FASEB Journal, 34: S1 (https://doi.org/10.1096/fasebj.2020.34.s1.05991)

Reprint requests: Philip Lazarus, Department of Pharmaceutical Sciences, College of Pharmacy and Pharmaceutical Sciences, Washington State University, Spokane, WA 99202-2131. Email: phil.lazarus@wsu.edu

DMD Fast Forward. Published on September 30, 2021 as DOI: 10.1124/dmd.121.000635
This article has not been copyedited and formatted. The final version may differ from this version.

Figure Legends

Figure 1. **UV and UPLC/MS chromatograms of EXE-GS and DHE-GS conjugates. Panel A**, EXE-GS standard with the parent ion spectrum (insert) for the peak at 1.20 min; **panel B**, EXE-GS conjugate formation by HLC with the parent ion spectrum (insert) for the peak at 1.20 min; **panel C**, EXE-GS conjugate formation with no enzyme added; **panel D**, 17β-DHE-GS standard with the parent ion spectrum (insert) for the peak at 0.80 min; **panel E**, 17β-DHE-GS conjugate formation by HLC with the parent ion spectrum (insert) for the peak at 0.90 min; **panel F**, 17β-DHE-GS conjugate formation with no enzyme added.

Figure 2. Cytosolic GST activities against EXE and 17β-DHE. Panel A, EXE-GS formation by recombinant GSTs; **panel B**, 17β-DHE-GS formation by recombinant GSTs. The GSTs were screened by incubating GSH with EXE (250 μM) using 2.5 ng/μl of purified recombinant protein. GS conjugates of EXE and DHE were detected using a Waters Xevo G2-S QToF mass spectrometer and expressed in ppm as described in the Materials and Methods.

Figure 3. Representative Michaelis-Menten curves of recombinant GSTs and HLC for the conjugation of EXE to EXE-GS (Panel A) and DHE to DHE-GS (Panel B). For EXE conjugation, experiments were performed using 1 μg/μL of HLC protein, 2.5 ng/μL of purified recombinant GSTA1, or 8 ng/μL of purified recombinant GSTM1 or GSTM3, with varying concentrations (2-250 μM) of EXE. For 17β-DHE conjugation, experiments

DMD Fast Forward. Published on September 30, 2021 as DOI: 10.1124/dmd.121.000635
This article has not been copyedited and formatted. The final version may differ from this version.

were performed using 2 µg/µL of HLC protein or 5 ng/µL purified recombinant GSTA1, with varying concentrations (2-250 µM) of 17β-DHE.

Figure 4. Western blot quantification of GSTA1, GSTM3 and GSTM1 in HLC. Panel A, serial dilution of HLC (25 - 6.25 µg of total protein) and purified recombinant GSTA1 (1 - 0.125 µg) used as standard, probed with a GSTA1-specific antibody; **panel B,** serial dilution of HLC (25 - 6.25 µg of total protein) and purified recombinant GSTM1 (0.25-0.03 µg) used as standard, probed with a GSTM1-specific antibody; **panel C**, serial dilution of HLC (25 - 6.25 µg of total protein) and purified recombinant GSTM1 (1 - 0.03 µg) used as standard, probed with a GSTM3-speciifc antibody. Western blots were conducted as described in the Materials and Methods.

Figure 5. Schematic of exemestane metabolism. AKR, aldoketoreductases; CBR, carbonyl reductase, CYP, cytochrome P450s; UGT, UDP glucuronyltransferase; GST, glutathione-S-transferases, GGT, gamma-glutamyl transferase.

DMD Fast Forward. Published on September 30, 2021 as DOI: 10.1124/dmd.121.000635
This article has not been copyedited and formatted. The final version may differ from this version.

Table 1. Kinetic analysis of GSTs against EXE and 17β-DHE.[a]

	EXE-GS			17β-DHE-GS		
	K_m (μM)	V_{max} (nmol·min^{-1}·mg^{-1})*	CL_{INT} (nl·min^{-1}·mg^{-1})*	K_m (μM)	V_{max} (nmol·min^{-1}·mg^{-1})*	CL_{INT} (nl·min^{-1}·mg^{-1})*
HLC	46 ± 12	0.044 ± 0.0067	0.0018 ± 0.00010	51 ± 14	0.0020 ± 0.00084	0.000037 ± 0.0000082
GSTA1	53 ± 17	4.7 ± 2.9	0.085 ± 0.043	32 ± 12	0.48 ± 0.13	0.017 ± 0.0067
GSTM3	99 ± 6.0	14 ± 1.4	0.14 ± 0.092	not active		
GSTM1	14 ± 4.1	0.43 ± 0.29	0.032 ± 0.017	not active		

[a] K_m, V_{max} and CL_{INT} are expressed as the mean ± S.D. of three independent experiments.
* Data are expressed per mg total cytosolic protein.

DMD Fast Forward. Published on September 30, 2021 as DOI: 10.1124/dmd.121.000635
This article has not been copyedited and formatted. The final version may differ from this version.

Table 2. Mean levels of GSTA1, GSTM1 and GSTM3 in human liver cytosols.

GSTA1	GSTM1	GSTM3
0.043 ± 0.0051[a]	0.0057 ± 0.00043[a]	not detected

[a] Data expressed as µg GST per µg of liver cytosolic protein.

Figure 1

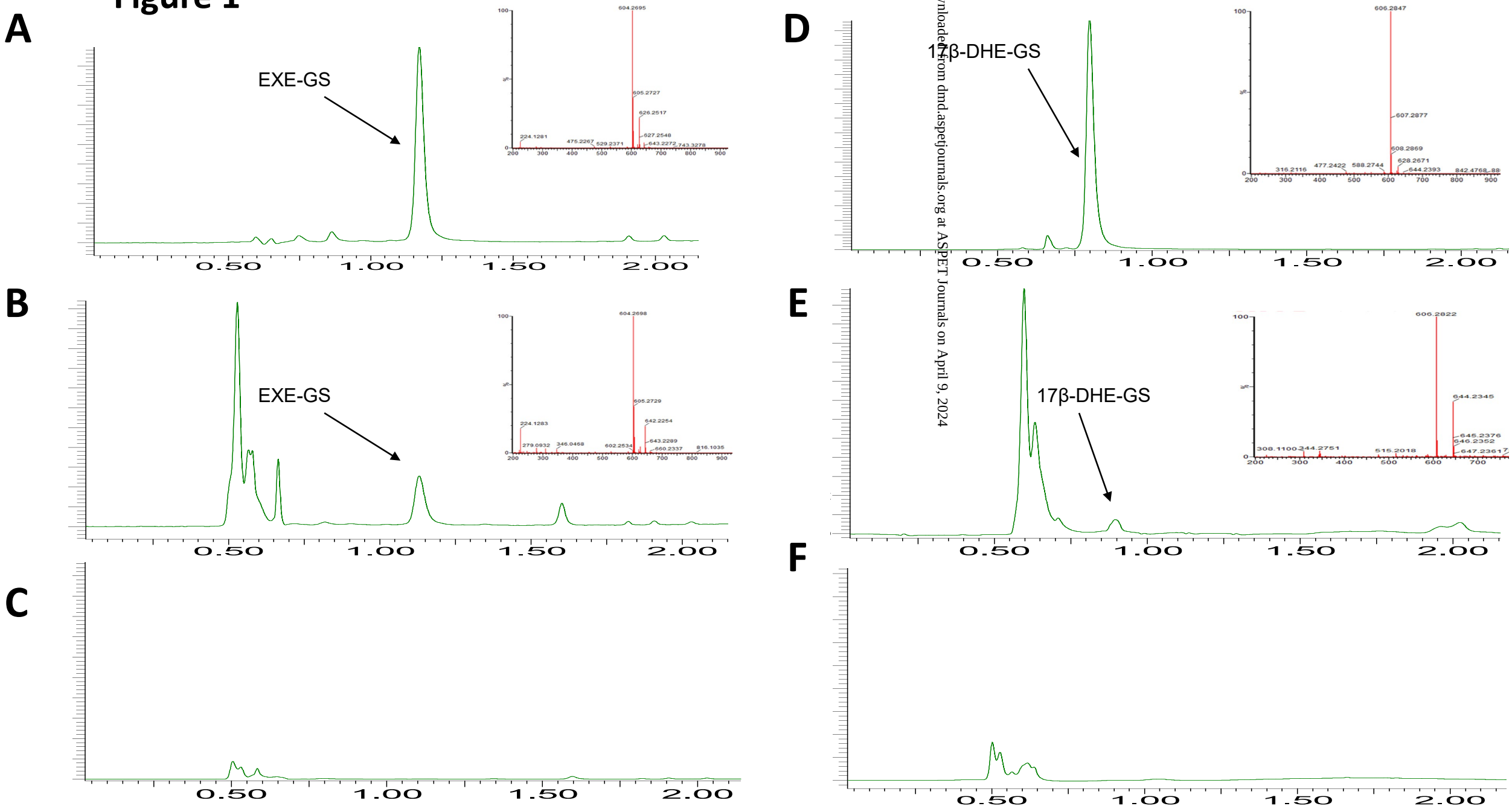

Figure 2

(A)

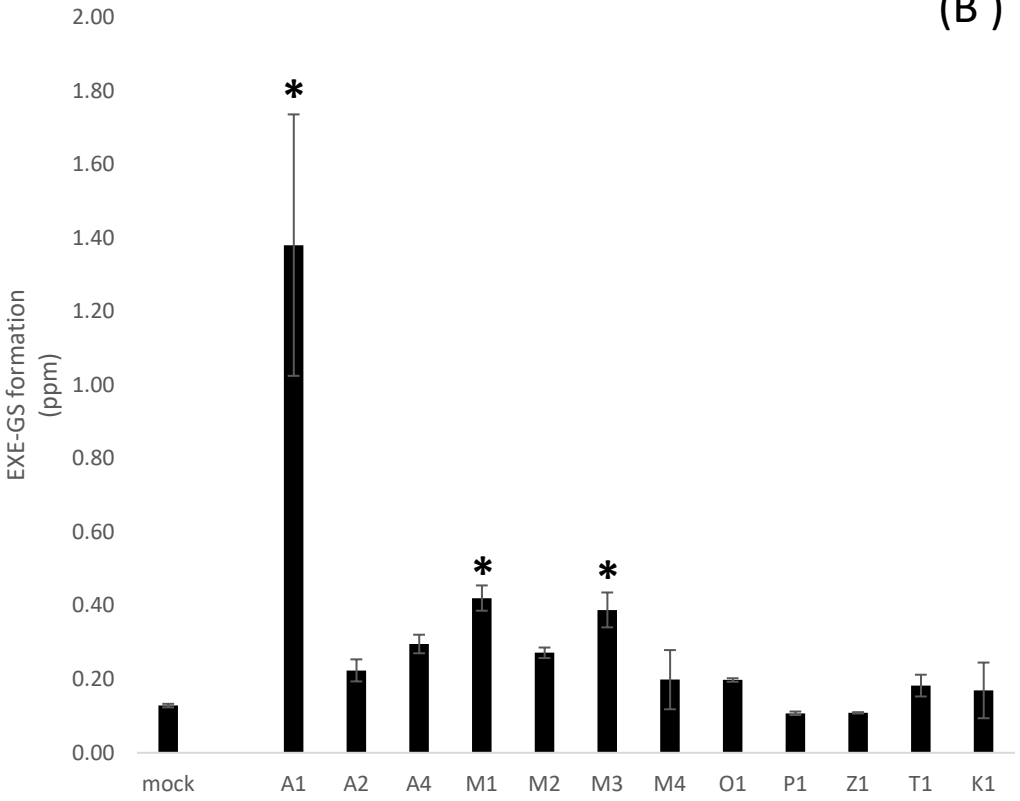

(B)

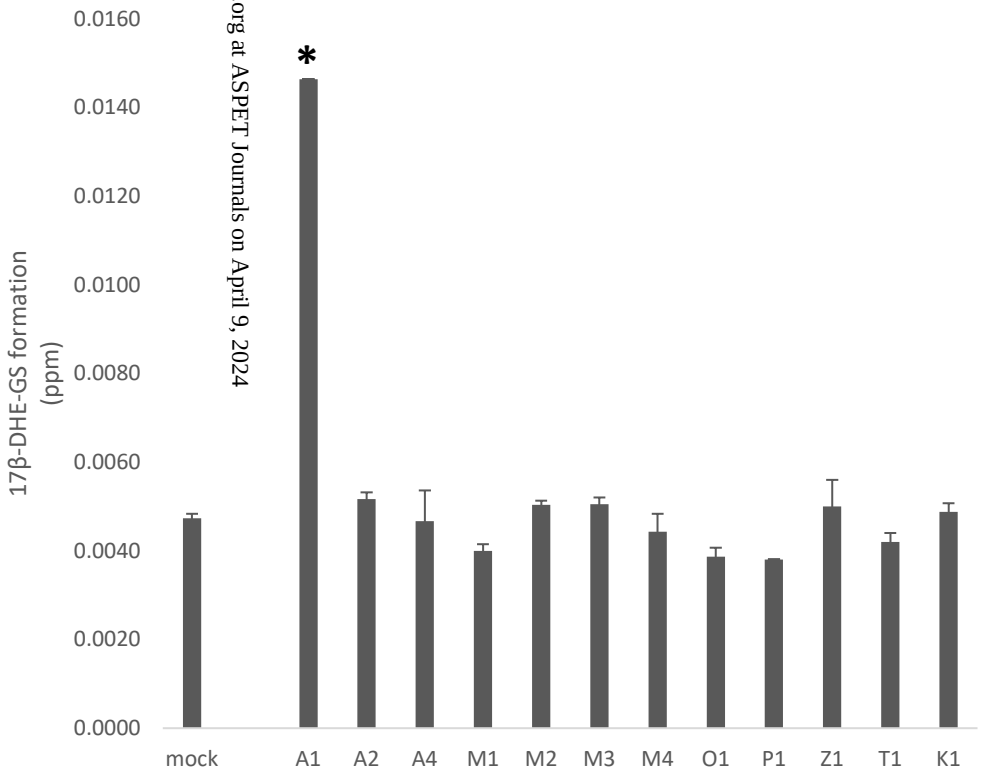

DMD Fast Forward. Published on September 30, 2021 as DOI: 10.1124/dmd.121.000635
This article has not been copyedited and formatted. The final version may differ from this version.

Figure 3

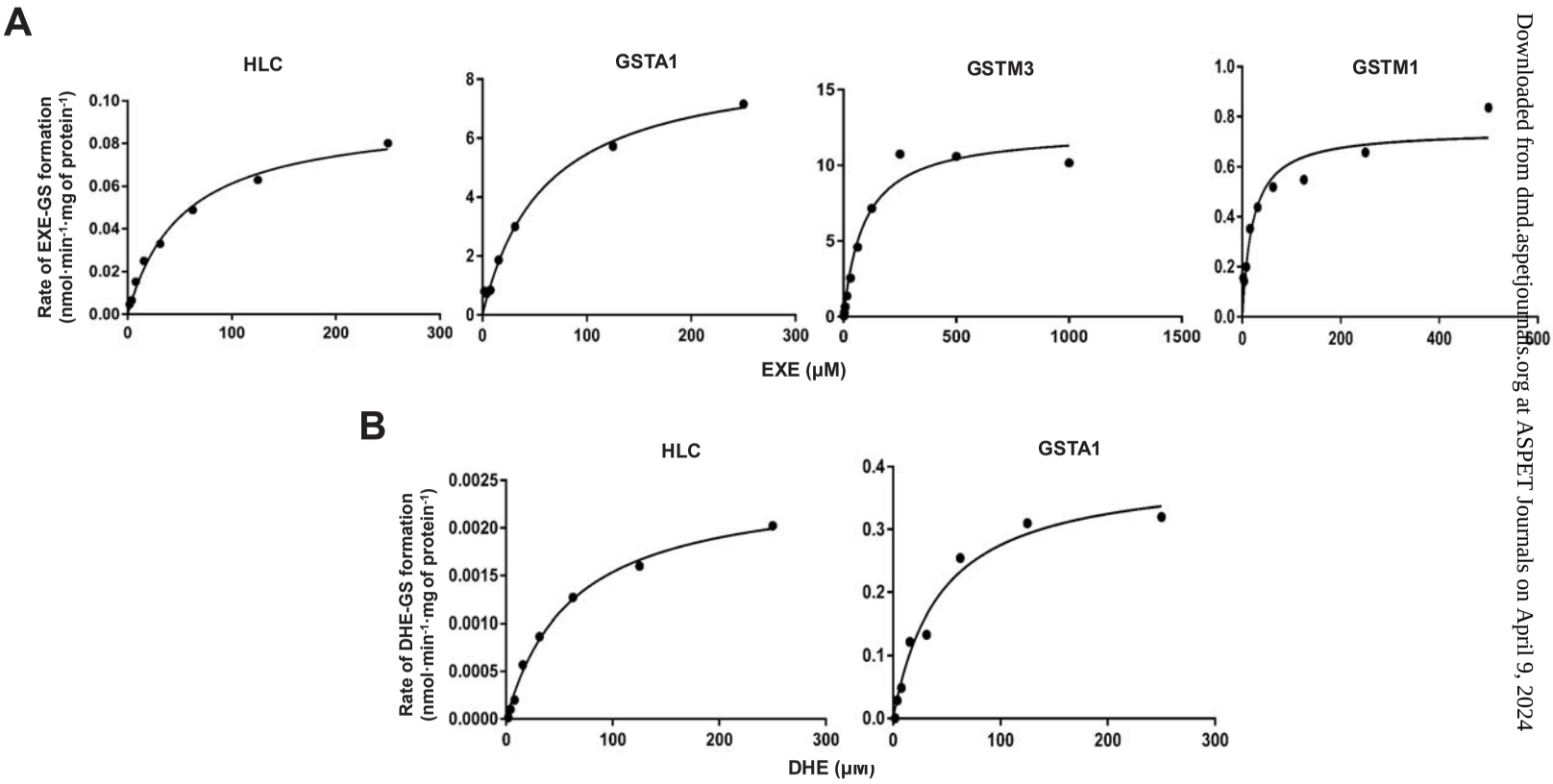

Figure 4

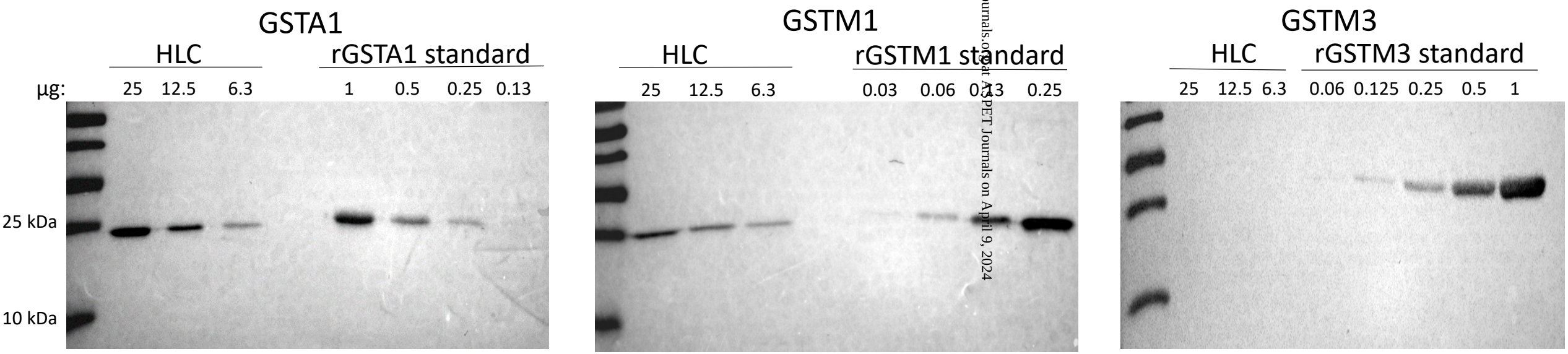

Figure 5